

# Energy based model to assess interfacial adhesion using a scratch test

Vincent Le Houérou · Christian Gauthier · Robert Schirrer

Received: 25 October 2007 / Accepted: 8 July 2008 / Published online: 9 August 2008  
© Springer Science+Business Media, LLC 2008

**Abstract** A common way to improve the scratch resistance of a sensitive surface is to coat it with a thin film. However, the substrate/thin film adhesion must be well controlled and measurable. The contribution of the present work is to propose a global energy balance model of the blistering process for the scratching of a substrate/thin film system, which permits one to determine the adhesion of the system. The adhesion can be measured by following the delaminated area as a function of the scratching distance during blistering. The particular case of an experimental stable blistering process was studied and the corresponding substrate/thin film adhesion was derived using the global energy balance model.

## Nomenclature

$V_{\text{tip}}$	Scratching velocity
$F_n, F_t$	Normal and tangential loads respectively
$T$	Temperature
$\Delta W$	Work provided by the loading indenter
$\Delta E_F$	Fracture energy
$\Delta E_D$	Energy released in dissipative phenomena other than fracture
$\Delta E_E$	Elastic energy
$d$	Scratching distance
$\mu_{\text{app}}$	Apparent friction coefficient
$\mu_{\text{local}}$	Local friction coefficient
$\Delta A_{\text{interf.}}$	Surface created at the interface
$\Delta A_{\text{coh.}}$	Surface created within the material

$\gamma_{\text{s-interf.}}$	Surface energy required to create 1 unit of interfacial new surface
$\gamma_{\text{s-coh.}}$	Surface energy required to create 1 unit of cohesive new surface
$\delta W_D$	Dissipative work (fracture excluded) per unit of scratching distance
$\delta W_E$	Elastic work per unit of scratching distance
$\delta W_{DP}$	Plastic deformation work of the system per unit of scratching distance
$\delta W_{DF}$	Work due to the true local friction
$\sigma_y$	Yield stress of the substrate
$S_t$	Cross section of the plastic zone in the scratching track left on the surface
$\Delta A_B$	Area of the blister
$p_{\text{atm}}$	Atmospheric pressure
$\bar{h}_a$	Average height of the blister
$\Delta A$	Delaminated area variation
$\Delta d$	Scratching distance variation
$W_{\text{idth}}$	Width of the blister as defined in Fig. 1
$R$	Radius of curvature of the indenter tip
$a$	Contact radius
$e$	Thickness of the film
$L_g$	Width of the groove
$\dot{\epsilon}$	Strain rate

## Introduction

Coatings are frequently used nowadays to improve the mechanical and tribological behavior of engineering and optical materials. However, the large number of parameters which influence this improvement demand a fundamental understanding of the roles played by the adhesion between the thin film and the underlying substrate and the mechanical properties of the two materials. The adhesion is characterized

V. Le Houérou (✉) · C. Gauthier · R. Schirrer  
Institut Charles Sadron (I.C.S.), CNRS UPR 022, 23 rue du  
Loess, BP 84047, 67034 Strasbourg cedex 2, France  
e-mail: lehouerou@ics.u-strasbg.fr

by the energy associated with an interfacial fracture between the film and the substrate. A wide variety of methods have been used to assess the adhesion of the coating [1–6], but none provides a unique value of the adhesive strength. The adhesion of the coating still remains to be successfully determined in a test which can reproduce the damage undergone by the coated surface during its real lifetime.

A single sliding contact scratch test has been widely used for some time now to obtain information (most of the time qualitative) about the scratch resistance of the material on the macro and micron scales (case of bulk materials) and on the sub-micron scale (case of thin film/substrate systems tested by nano-scratching) [7–9]. As the sliding contact nevertheless generates a complicated stress field, both materials can undergo compression, traction, or hydrostatic pressure, while the interface can be submitted to shear stress and the coating to buckling or other stresses. In addition, the behavior of each material plays a fundamental role and greatly complicates the mechanical models. Thus, sliding or scratching contacts, especially on coated surfaces, are not easy to understand, nor to simulate or predict [10].

To model the surface damage of a coated sample, the fracture mechanics approach using the energy release rate  $G_c$  to characterize the interfacial toughness of the material has met with quantitative success in several cases [2, 4]. The load at which failure occurs, termed the critical load, is sometimes used to assess qualitatively the coating/substrate adhesion [11, 12]. Otherwise, another promising quantitative approach employs energy balance modeling to eliminate the complexity of the problem. Volinsky et al. [5] have developed an energy balance model for the buckling of a film which may be summarized as:

$$W_{A,P} = W_A + U_f + U_s + U_{\text{fric}} \quad (1)$$

with  $W_{A,P}$  the measured work of adhesion,  $W_A$  the true work of adhesion,  $U_f$  and  $U_s$  the energies spent by plastic deformation of the film and the substrate, respectively, and  $U_{\text{fric}}$  the energy spent by friction.

The present paper proposes a global energy balance model which permits, among other things, quantitative assessment of the coating/substrate adhesion during scratching. The model is applied to an analysis of the steady state growth of blistering.

### The energy balance model

The following model may be used for single-coated or bulk materials, multi-layered or property-gradient materials so long as their characteristics are known. The variational form of the energy balance, i.e., considered between two distinct arbitrary time points during the blistering process, can be written as follows:

$$\Delta W = \Delta E_F + \Delta E_D + \Delta E_E \quad (2)$$

$\Delta W$  is the work provided by the loading indenter, while  $\Delta E_F$  is the fracture energy which may correspond to fracture within the film and/or the substrate or to fracture at the film/substrate interface in a delamination phenomenon.  $\Delta E_D$  is the energy released in other dissipative phenomena not taken into account in the other terms of Eq. 2. This extra dissipation may be due to plastic deformation of the substrate and/or the thin film, or to local friction between the surface of the sample and the indenter, etc.  $\Delta E_E$  is the elastic energy due to reversible contributions. The loading indenter, for instance, inputs elastic strain energy into the material system. Owing to the sliding process, this energy is constant during the test since the normal force remains constant. Actually, as the material elastically deforms in front of the sliding indenter, it elastically relaxes behind and the resulting elastic energy is nil in the variational energy balance. Nevertheless, the elastic strain energy stored in the thin film to keep it in a buckled shape, for example, is also included in the  $\Delta E_E$  term and will be further discussed (§ 3.2). Reversible contributions like the work of the atmospheric pressure on a blister do not appear in the energy balance since these are rigorously written as the equilibrium of variations of the energies considered. Eq. 2 is somewhat similar to the variational form of Eq. 1 cited in the introduction.

Let  $d$  be the scratching distance covered by the indenter in the lapse of time considered in the variational energy balance. The period of interest in the present case is a part of the time elapsed between the initiation of the blister and the end of the test (both excluded).

The expression describing the work corresponding to the indenter loading is clearly:

$$\Delta W = F_t d = \mu_{\text{app}} F_n d \quad (3)$$

with  $F_n$  and  $F_t$  the normal and tangential loads, respectively, and  $\mu_{\text{app}}$  the apparent friction coefficient, i.e.,  $\mu_{\text{app}} = F_t/F_n$ .

The fracture energy  $\Delta E_F$  may be due to: (i) interfacial fracture (between the thin film and the substrate) and/or (ii) cohesive fracture within the material (film and/or substrate). Hence, the fracture energy may be written as:

$$\Delta E_F = 2(\Delta A_{\text{interf.}} \gamma_{s\text{-interf.}} + \Delta A_{\text{coh.}} \gamma_{s\text{-coh.}}) \quad (4)$$

where  $\Delta A_{\text{interf.}}$  (respectively,  $\Delta A_{\text{coh.}}$ ) is the area created at the interface (resp., within the material) and  $\gamma_{s\text{-interf.}}$  (resp.,  $\gamma_{s\text{-coh.}}$ ) is the surface energy required to create 1 unit of interfacial (resp., cohesive) new surface.

The energy dissipation  $\Delta E_D$  may be divided into as many terms as there are dissipative sources, or simply written as a function of the scratching distance  $d$ :

$$\Delta E_D = \delta W_D d \quad (5)$$

with  $\delta W_D$  the associated dissipative work per unit of scratching distance.

The stored elastic energy  $\Delta E_E$  can be written in its elementary form, introducing the associated elastic work per unit of scratching distance  $\delta W_E$ :

$$\Delta E_E = \delta W_E d \tag{6}$$

Finally, the energy balance in the general case is given by:

$$\mu_{app} F_n = \frac{2}{d} (\Delta A_{interf.} \gamma_{s-interf.} + \Delta A_{coh.} \gamma_{s-coh.}) + \delta W_D + \delta W_E \tag{7}$$

### Experimental blistering process

#### Description of the experimental blistering process

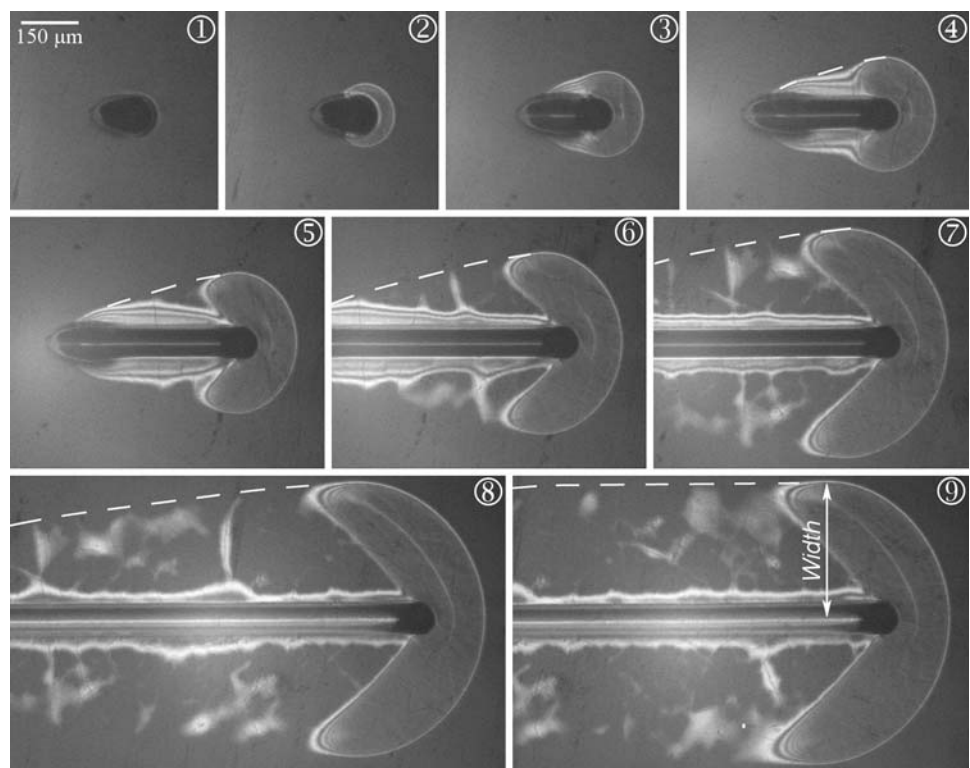
The experimental procedure must generate a blister as large as possible in order to have convenient images to analyze. A blister which grows slowly and extensively during scratching is therefore suitable, and the newly identified “crescent blister” (compared to blister kinetics reported in literature [13]) illustrated in Fig. 1 and described previously [14] was chosen.

Blistering was obtained on a coated sample scratched at 80 °C with a spherical indenter of radius 116 μm at a scratching speed of 10 μm/s. The sample was an amorphous

polycarbonate substrate coated (by the dip coating technique) with a 3.5 μm thick thermoset matrix filled to about 20% of its volume with nano-sized silica particles (about 10 nm in diameter). Since the adherence was not optimized during the coating procedure, the interfacial strength was expected to be weak. The scratch test apparatus has been fully described elsewhere [15]. The normal load  $F_n$  (kept constant), tangential load  $F_t$ , scratching speed  $V_{tip}$ , and temperature  $T$  are continuously monitored and recorded during experiments. A built-in microscope allows in situ observation of the indenter/sample contact through the transparent specimen.

The blistering process can be described with the help of the images shown in Fig. 1 which were taken from the video sequence of a scratching experiment. Chronologically, the interfacial crack triggered by buckling corresponds to initiation of the blister (see picture ② in Fig. 1), after which a large delaminated circular-shaped blister appears ahead of the indenter and at the outer edges of the scratching track left on the surface (see pictures ② and ③). After a few micrometers of indenter displacement, the rear part of the blister separates from the scratching track on both sides (see pictures ④ and ⑤). This unusual-shaped blister (called a “crescent” blister) moves with the indenter and becomes progressively larger (see pictures ⑤ to ⑩). One should note that the thin film sticks back onto the surface of the sample behind the blister. This sticking-back phenomenon is not incompatible with the global

**Fig. 1** Chronological sequence of the crescent blistering process as the indenter scratches the material. The dashed curves delimit the area of the thin film which sticks back onto the substrate. The width of blister is shown in the picture ⑩



energy balance model because the energy returned to the system is of chemical origin, and therefore does not have to appear in the mechanical energy balance given in § 2. The stuck-back surface together with the blistered surface constitutes the total delaminated area, which has the approximate shape of a sector of a circle (see pictures ④ to ⑧) with an apparent radius corresponding to the scratching distance from the starting point of blistering and an average half angle defined by the scratching direction and the dashed curve drawn in Fig. 1. When the blister has reached a certain size, it propagates with the indenter without increasing further in size (see picture ⑨). Thus, propagation of the crescent blister ends when the test finishes or when cohesive cracking suddenly occurs within the film. In the latter case, the final damage pattern is a chip ahead of the indenter and a large delaminated surface behind as the cracks propagate and demarcate part of the blister.

### The energy balance

#### Work of the indenter: $\Delta W$

The work  $\Delta W$  provided by the indenter during scratching may be written as in Eq. 3, and  $\Delta W$  is easily accessible since  $d$ ,  $F_n$ , and  $F_t$  are continuously recorded during a test. The experimental apparent friction coefficient, given by the ratio of  $F_t$  to  $F_n$ , is roughly 0.25 and constant throughout the test. Thus, Eq. 3 reduces to a proportional relation between the work of the indenter and the scratching distance.

#### Fracture energy: $\Delta E_F$

In the present case, the fracture energy  $\Delta E_F$  corresponds to the energy dissipated by growth of the blister arising from fracture at the interface between the substrate and the thin film. Since during the blistering process neither blister initiation nor eventual final cracking within the film are taken into consideration, Eq. 4 reduces to the first term corresponding to the interfacial phenomenon:

$$\Delta E_F = 2\Delta A_{\text{interf.}} \gamma_{\text{s-interf.}} \quad (8)$$

Therefore,  $\Delta E_F$  is expressed as a function of the interfacial energy  $\gamma_{\text{s-interf.}}$  of the substrate/thin film system and the fracture area  $\Delta A_{\text{interf.}}$ , this delaminated area being an unknown variable in the equation. The areas of interest were quantified by image analysis of the video sequence and in Fig. 2 the total delaminated area is plotted as a function of the scratching distance. After its initiation, the growth of the blister proceeds in two different states. Firstly, a transient state where the total delaminated area seems to follow a polynomial evolution with respect to the scratching distance. According to Fig. 1 (see pictures ④ to

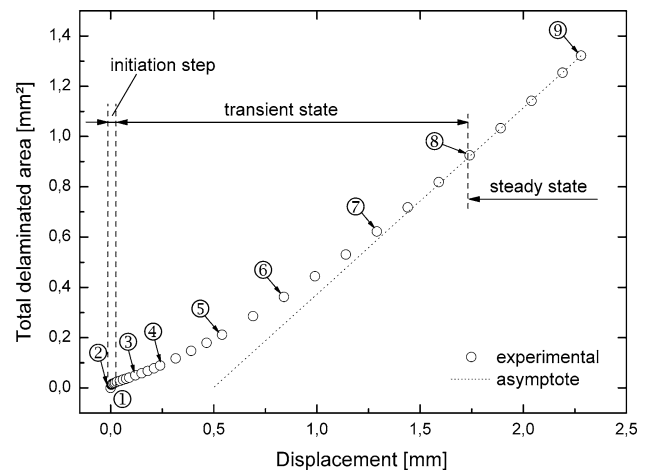


**Fig. 2** Total delaminated area as a function of the scratching distance. The initiation step and the transient and steady states are defined and indexes ① to ⑨ relating to Fig. 1 are indicated for convenience

⑧), this polynomial evolution is coherent with the shape of the delamination (approximately a sector of a circle of radius equal to the scratch length). Secondly, a steady state where the total delaminated area follows a linear evolution, as shown by the asymptote in Fig. 2. This state corresponds to the propagation of a stabilized blister with constant shape and size (see picture ⑨ in Fig. 1).

The quantitative energy balance model will be applied only from the beginning of the transient state (step ② in Figs. 1 and 2) to the end of the scratching process, excluding the initiation step from the analysis for the sake of simplicity. Moreover, as reported by Dupeux [16], the initiation of interfacial cracking requires an energy which would appear to be hardly reproducible. Hence, the propagation of the delaminated area and the evolution of the energy involved can be more precisely determined in the transient and steady states.

#### Dissipated energy: $\Delta E_D$

As mentioned in § 2, the associated dissipative work per unit length of displacement (i.e., infinitesimal variation in space)  $\delta W_D$  given in Eq. 5 may be divided into as many terms as there are dissipative sources. In the present case, it can be reduced in a first approximation to two terms:  $\delta W_{DF}$  corresponding to the plastic deformation of the system and  $\delta W_{DF}$  corresponding to the contribution of the true local friction. The coating deposited on the polycarbonate substrate is known to have a large elastic domain relative to the substrate. As a consequence, the plastic energy dissipated in the coating will be negligible as compared to the plastic energy dissipated in the substrate. To determine the dissipative work arising from the plasticity of the substrate, the volume of the residual plastic zone must be estimated

since it contains the work dissipated by plasticity in the material due to the normal and tangential contributions of the loading. The plastic work spent per unit length of scratching may be written as:

$$\delta W_{DP} = \sigma_y S_t \tag{9}$$

with  $\sigma_y$  the yield stress of the substrate and  $S_t$  the cross section of the plastic zone in the scratching track left on the surface.

The term  $\delta W_{DF}$  arises from the true local friction at the indenter/coating interface and also from friction between the coating and substrate. However, since in situ visualization shows that the thin film does not slide on the substrate, the latter contribution does not exist in our experiments. As a result, the friction contribution may be quantified as:

$$\delta W_{DF} = F_n \mu_{local} \tag{10}$$

which gives in our case:

$$\Delta E_D = (\sigma_{yield} S_t + F_n \mu_{local}) d \tag{11}$$

*Elastic energy:  $\Delta E_E$*

The elastic energy needed to maintain a blister in its buckled shape appears in the global energy balance in the transient growth state of the blister. Actually, in the transient state the blister area grows linearly, whereas the total delaminated area scales as the square of its apparent radius, which is the displacement since the start of the blistering process. This proportional growth of the blister area in the transient state has also been demonstrated by direct measurement [14]. Since in this state the blister grows linearly, part of the elastic energy is continuously stored in the growing buckled blister and thus appears in the global energy balance. The amount of energy is easily estimated as follows: the maximum amount of elastic strain energy stored to keep the film in its buckled shape is the opposite of the work spent by the atmospheric pressure to maintain it. The energy dissipated in deformation within the film can be neglected to a first order approximation in view of the low Young’s modulus of the coating. Hence, in the present case the elastic strain energy  $\Delta E_{E-Film}$  stored in the film can be approximated by:

$$\begin{aligned} \Delta E_{E-Film} &= \Delta A_B p_{atm} \bar{h}_a d && \text{if the transient state is part of} \\ & && \text{the analysis} \\ \Delta E_{E-Film} &= 0 && \text{otherwise} \end{aligned} \tag{12}$$

where  $\Delta A_B$  is the area of the blister,  $p_{atm}$  the atmospheric pressure, and  $\bar{h}_a$  the average height of the blister,  $\bar{h}_a$  being a function of time and location.

On the contrary, the elastic energy needed to keep the blister buckled during the steady state of its growth does

not appear in the energy balance because the blister propagates, while its buckled shape remains the same.

*Global energy balance*

The global energy balance (see Eq. 7) reduces in the present case to:

$$F_t = \frac{2\Delta A_{interf.} \gamma_{s-interf.}}{d} + \delta W_D + \delta W_E \tag{13}$$

with the notations described above.

**Results and discussion**

Determination of the local friction using the global energy balance model

First of all, an interesting result appears when writing the global energy balance of Eq. 13 in the particular case where cracking does not occur (bulk or coated elasto-plastic material):

$$F_t = \delta W_{DF} + \delta W_{DP} \tag{14}$$

Using Eq. 10 and Eq. 9, Eq. 14 divided by  $F_n$  gives:

$$\mu_{app} = \mu_{local} + \frac{\sigma_{yield} S_t}{F_n} \tag{15}$$

where  $\mu_{app}$  is the apparent friction coefficient.

Equation 15 can constitute a simple way to estimate the local friction coefficient  $\mu_{local}$  of the contact if  $F_n$  and  $\mu_{app}$  are measured and the yield stress of the material is known, using for instance Eq. 15 which requires only the width of the residual scratching track.

Estimation of the interfacial adhesion  $\gamma_{s-interf.}$  and discussion on St estimation

In the case of the present coated polycarbonate, the energy balance model provides a simple expression for the adhesion  $\gamma_{s-interf.}$  which depends on the normal load, the delaminated area, and the scratch length (see Eq. 13).

The elastic strain energy stored in the film is estimated from Eq. 12:

$$\begin{aligned} \Delta E_{E-Film} &= 200000 \times 10^{-12} \times 1 \times 10 \times 10^{-6} \\ &= 2 \times 10^{-12} \text{ J} \end{aligned}$$

This calculation confirms that the elastic strain energy can be neglected in Eq. 13, which can be re-written as:

$$\Delta A_{interf.} = \frac{d}{\gamma_{s-interf.}} f(F_n, \mu_{app}, \mu_{local}, \sigma_{yield}, S_t) \tag{16}$$

where  $f$  is a function depending on the variables in brackets.

As explained in § 3.2, the initiation of the blister during the first micrometers of the indenter advance is not included in the model. Eq. 16 indicates that the delaminated area  $\Delta A_{\text{interf.}}$  is theoretically a linear function of the scratch length  $d$ . Thus, the graphic representation of this linear function having the slope  $f(F_n, \mu_{\text{app}}, \mu_{\text{local}}, \sigma_{\text{yield}}, S_t)/\gamma_{\text{s-interf.}}$  shown in Fig. 2 as the asymptote of the experimental curve is the upper possible boundary of blister propagation. One may note that this boundary is derived from a propagation criterion and not from an initiation criterion as the latter phenomenon is excluded from the model.

As a consequence, the delaminated area during the steady state (i.e., for large values of scratching distance) follows the linear function described in Eq. 16. The slope is about  $741 \times 10^{-3}$  mm (obtained by a linear fit on Fig. 2) and gives the maximal propagation rate, which enables determination of the interfacial adhesion  $\gamma_{\text{s-interf.}}$ . Finally, only the slope of the maximal propagation rate is required to compute the interfacial adhesion  $\gamma_{\text{s-interf.}}$ . Moreover, one should note that this latter value is easy to assess in the case of a stabilized blister propagation. The considered slope is given by:

$$\frac{\Delta A}{\Delta d} = \frac{W_{\text{idth}} \Delta d}{\Delta d} = W_{\text{idth}} \quad (17)$$

where  $\Delta A$  is the delaminated area variation considered in the steady state propagation for the slope calculation,  $\Delta d$  is the corresponding length, and  $W_{\text{idth}}$  is the width of the blister as defined in Fig. 1. In the end, the slope value is equal to the width of the blister in the steady state propagation.

The estimation of the cross section of the plastic zone  $S_t$  is a delicate point. Different methods are presented and discussed in this part. First of all, the boundary of the plastic zone can be considered semi-circular with a radius equal to the contact radius  $a$  (see the hatched area in Fig. 3), as is commonly assumed. The plastic imprint is approximated by the shape of the indenter and the thin film is not taken into account in the plastic volume as it is probably purely elastically deformed. The cross sectional area  $S_t$  obtained, which is an approximation, is given by:

$$S_t = \frac{\pi a^2}{2} - R^2 \arcsin \frac{a}{R} + a \sqrt{R^2 - a^2} - 2\pi a e \quad (18)$$

Pile-ups are largely ignored in Eq. 18 and in situ visualization shows that this assumption is an approximation. Actually, the scratch reported in Fig. 1 is not a fully plastic scratch as defined by Bucaille et al. [17], since push pad and lateral pile-ups seem to be light. It results that the cross section of the plastic zone in the case of the coated substrate is probably greatly smaller than in the case of the

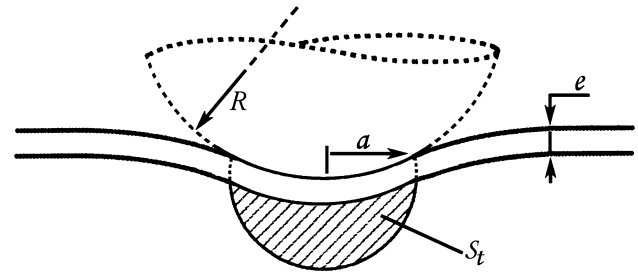


Fig. 3 Nomenclature for calculation of the plastic cross section  $S_t$

approximation given by Eq. 18 related to Fig. 3. Finally, an ultimate way to investigate the size of the plastic zone may be to use Finite Elements modeling. Major developments remain necessary to model completely the problem that consists in the scratching of an elastic coating deposited on an elasto-plastic substrate with cracking occurrence in the interface and friction consideration. The size of the cross section of the plastic zone will be discussed at the end of this part.

The adhesion  $\gamma_{\text{s-interf.}}$  was computed from this slope and Eq. 16:  $F_n$  was roughly 0.45 N,  $\mu_{\text{app}}$  was roughly 0.25, and  $\mu_{\text{local}}$  was estimated to be 0.13 using the method described by Lafaye et al. [18]. It is important to note that the mean scratch strain rate given by  $V_{\text{tip}}/L_g$  [15] (with  $L_g$  the width of the groove) was equal approximately to  $0.12 \text{ s}^{-1}$ . Thus,  $\sigma_y$  of the polycarbonate at  $80^\circ \text{C}$  was approximately 60 MPa at  $\dot{\epsilon} = 0.12 \text{ s}^{-1}$ , the half-width of the residual scratching track was about  $40.5 \mu\text{m}$ , the indenter was a spherical diamond tip of radius  $116 \mu\text{m}$ . Two furthest situations can be considered. Firstly, if no cracking at the interface is considered, the energy spent in plastic deformation will be maximum. It results in an upper bound of the plastic zone size:  $922 \mu\text{m}^2$  of cross section. In comparison, Eq. 18 gives  $S_t = 1360 \mu\text{m}^2$ . This confirms that the analytical method overestimates greatly the real plastic size. Secondly, if no energy is considered to be spent in plastic deformation of the material, Eq. 16 gives an upper bound of the adhesion about  $37 \text{ J/m}^2$ . This is a consistent result since the adhesion was expected to be weak and an interaction of this order of magnitude should be compared to the Van der Waals adhesion, typically about  $3 \text{ mJ/m}^2$ , or the adhesion corresponding to cohesive fracture in polymers, typically about  $3,000 \text{ J/m}^2$ .

The linear relation between blister area and scratch length also shows that the blister reaches a stable width on the surface of the sample while a constant amount of work is continuously provided to the blistering system during the scratching process. Hence, the transient state corresponds to the scratching distance which the material needs to attain stably shaped blister propagation. Since this accommodation minimizes the energy spent during advance of the crack tip, the evolution of the delaminated area (see Fig. 2)

during the transient state remains below the maximal propagation rate. The energy lost in the transient state, understand the energy not used for optimal propagation of the blister, is dissipated in the interfacial cracking process which tends to its minimal energy as it reaches the steady state and the final shape of blister propagation.

### Blister propagation and cracking

#### *Transient state blister propagation*

The global energy balance model is convenient to describe a steady state propagating blister. However, this steady state is not easy to attain as the propagation of the blister usually ends suddenly due to cracking within the film. The evolution of the propagation of the blister (see Fig. 2) is reproducible in different tests, but cracking within the film takes place randomly and is unpredictable. This means that most of the time, under the same conditions, the blistering process is stopped by cracking in the film at a random time point before the total delaminated area has reached its steady state growth phase during which the blister propagates with a stabilized shape and size. The consequence is an incomplete record of the delaminated area as a function of indenter displacement, often interrupted in the transient state and hence in the polynomial part of the curve (see Fig. 4). It nevertheless remains possible to obtain information about the adhesion from this kind of interrupted test. The slope of the curve to the final fracture point is evidently less than the maximal blister propagation rate which should have been measured during the corresponding steady state propagation. Thus, using Eq. 16, this corresponding slope derived from the interrupted test gives an upper bound of the interfacial adhesion through the determination of the function  $f^*$  (instead of  $f$ ).

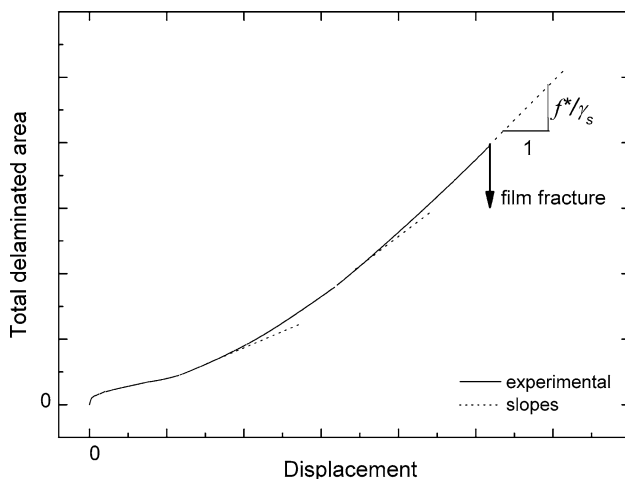


**Fig. 4** Estimation of an upper bound of interfacial adhesion from an incomplete scratch test

### *Blistering under reduced load*

As explained above, long steady state propagation of a blister is not easy to obtain experimentally. In such experiments the applied normal load is kept constant during scratching and equal to the load necessary to initiate the interfacial crack. Since the load needed to initiate blistering is greater than that needed to propagate the blister, the latter spreads widely and its large size increases considerably the probability that cohesive cracking will occur within the thin film before the steady state has been reached. A simple way to avoid this problem is to initiate the interfacial crack with a sufficient load and then decrease the load immediately in order to obtain a steady state propagating blister with reasonable dimensions. The drop in normal load reduces the slope of the propagation rate in Fig. 2 and 4, i.e., decreases the function  $f$  in Eq. 16. The maximal blister propagation rate (steady state) is reached after a shorter scratching distance (shorter transient state), providing a small stabilized blister. Moreover, these blisters are easy to reproduce, and there is no premature interruption of the test due to cohesive fracture within the film.

### Conclusion

The contribution of the present work is to propose a way of determining the adhesion between a coating and its underlying substrate using a scratch test, which is able to reproduce conditions similar to those encountered by the material in real life.

A global energy balance model of the blistering process has been developed for the scratching of a substrate/thin film system. It permits one to assess the adhesion of the system by following the evolution of the total delaminated area as a function of the scratching distance. The model was applied to an experimental stable blistering process and led to a calculated upper bound of adhesion of about  $37 \text{ J/m}^2$ , consistent with the expected adhesion. The difficulty of this method has been pointed out and consists in the estimation of the size of the plastic zone induced by scratching. The establishment of a complete Finite Element model of the system would be helpful to solve the problem more precisely.

**Acknowledgement** The authors would like to thank C. Robert for his preliminary experimental work.

### References

1. Bull SJ, Berasetegui EG (2006) Tribol Int 39:99. doi:[10.1016/j.triboint.2005.04.013](https://doi.org/10.1016/j.triboint.2005.04.013)

2. Hutchinson JW, Suo Z (1992) *Adv Appl Mech* 29:63
3. Mittal KL (1978) Adhesion measurement of thin films, thick films and bulk coatings. STP 640, ASTM, Philadelphia, PA
4. Thouless MD (1998) *Eng Fract Mech* 61:75. doi:[10.1016/S0013-7944\(98\)00049-6](https://doi.org/10.1016/S0013-7944(98)00049-6)
5. Volinsky AA, Moody NR, Gerberich WW (2002) *Acta Mater* 50:441. doi:[10.1016/S1359-6454\(01\)00354-8](https://doi.org/10.1016/S1359-6454(01)00354-8)
6. Ritter JE, Lardner TJ, Rosenfeld L, Lin MR (1989) *J Appl Phys* 66:3626. doi:[10.1063/1.344071](https://doi.org/10.1063/1.344071)
7. Bull SJ, Rickerby DS (1990) *Surf Coat Tech* 42:149. doi:[10.1016/0257-8972\(90\)90121-R](https://doi.org/10.1016/0257-8972(90)90121-R)
8. Perry AJ (1983) *Thin Solid Films* 107:167. doi:[10.1016/0040-6090\(83\)90019-6](https://doi.org/10.1016/0040-6090(83)90019-6)
9. Kriese MD, Boismier DA, Moody NR, Gerberich WW (1998) *Eng Fract Mech* 61:1. doi:[10.1016/S0013-7944\(98\)00050-2](https://doi.org/10.1016/S0013-7944(98)00050-2)
10. Holmberg K, Laukkanen A, Ronkainen H, Wallin K, Varjus S, Koskinen J (2006) *Surf Coat Tech* 200:3793. doi:[10.1016/j.surfcoat.2005.03.040](https://doi.org/10.1016/j.surfcoat.2005.03.040)
11. Blee MH, Winkelmann GB, Balkenende AR, den Toonder MJM (2000) *Thin Solid Films* 359:1. doi:[10.1016/S0040-6090\(99\)00729-4](https://doi.org/10.1016/S0040-6090(99)00729-4)
12. Bull SJ (1997) *Tribol Int* 30:491. doi:[10.1016/S0301-679X\(97\)00012-1](https://doi.org/10.1016/S0301-679X(97)00012-1)
13. Li J, Beres W (2007) *Can Metall Q* 46:155
14. Le Houérou V, Robert C, Gauthier C, Schirrer R (2008) *Wear* 265:507. doi:[10.1016/j.wear.2007.11.019](https://doi.org/10.1016/j.wear.2007.11.019)
15. Gauthier C, Schirrer R (2000) *J Mater Sci* 35:2121. doi:[10.1023/A:1004798019914](https://doi.org/10.1023/A:1004798019914)
16. Dupeux M (2004) *Mecanique Indust* 5:441. doi:[10.1051/meca:2004044](https://doi.org/10.1051/meca:2004044)
17. Bucaille JL, Gauthier C, Felder E, Schirrer R (2006) *Wear* 260:803. doi:[10.1016/j.wear.2005.04.007](https://doi.org/10.1016/j.wear.2005.04.007)
18. Lafaye S, Gauthier C, Schirrer R (2005) *Tribol Int* 38:113. doi:[10.1016/j.triboint.2004.06.006](https://doi.org/10.1016/j.triboint.2004.06.006)